

Adsorption and Photoactivity of Tetra(4-carboxyphenyl)porphyrin (TCPP) on Nanoparticulate TiO₂

Suman Cherian and Carl C. Wamsler*

Department of Chemistry, Portland State University, Portland, Oregon 97207-0751

Received: December 22, 1999

Tetra(4-carboxyphenyl)porphyrin (TCPP) adsorbs strongly onto nanoparticulate TiO₂ and serves as an efficient photosensitizer for solar-energy conversion by TCPP-sensitized TiO₂ electrodes. Nanoparticulate TiO₂ electrodes were prepared from Degussa P25 TiO₂ powder in the standard manner for a Grätzel cell. Adsorption studies of TCPP onto these sintered TiO₂ electrodes gave a saturation surface coverage of 47 μmol/g. Adsorption studies of TCPP onto colloidal dispersions of Degussa P25 in ethanol gave a saturation surface coverage of 77 μmol/g. The difference between the saturation coverages is attributed to the reduction of the available surface area in the TiO₂ films after sintering, from 55 m²/g as a free colloid to about 34 m²/g as a sintered electrode. The nature of the binding of TCPP onto the TiO₂ electrodes was investigated using X-ray photoelectron spectroscopy (XPS) and Resonance Raman Spectroscopy (RRS). In the XPS spectra of TiO₂ with adsorbed TCPP, the O (1s) and Ti (2p_{3/2}) peaks of TiO₂ were shifted to a higher binding energy value, by about 0.3 eV, and the O (1s) and N (1s) peaks of TCPP were shifted to a higher binding energy, by about 0.7 eV. Upon adsorption of TCPP, one of the Ti (2p_{3/2}) peaks of TiO₂ disappeared, suggesting complexation and removal of surface states. The RRS results indicated that for cases in which TCPP was adsorbed onto TiO₂ films from ethanolic solutions of about 1 μM concentration, the porphyrin spectrum showed distinctive interactions with the surface, but for cases in which it was adsorbed from higher concentrations, the RRS spectra were similar to spectra of TCPP powder, indicating the dominance of porphyrin–porphyrin interactions. We conclude that lateral interactions between adsorbed TCPP are significant upon adsorption from all but the lowest (micromolar) initial concentrations. Photovoltaic cells with TCPP-sensitized TiO₂ electrodes gave good solar-energy conversion efficiencies. At light simulating one sun (AM 1.5), a cell sensitized by TCPP gives a short-circuit photocurrent of about 6 mA/cm² and an open-circuit photopotential of 485 mV. The incident photon-to-current conversion efficiency was 55% at the Soret peak and 25–45% at the Q-band peaks; the cells have a fill factor of 60–70% and an overall energy conversion efficiency of about 3%.

Introduction

The photosensitization of wide band-gap semiconductors has been an active area of research, especially since the development of the high-efficiency solar cell based on dye-sensitized nanocrystalline TiO₂ films.^{1–6} The porous nature of the film increases the surface area by a factor of about 1000, leading to an efficient light harvesting by just one monolayer of the dye. Some of the dyes that have been used as sensitizers are substituted bipyridyl complexes of ruthenium, chlorophyll derivatives, related natural porphyrins, and other natural dyes.^{7–9} In these dye-sensitized cells, efficient charge separation takes place due to electron injection from the excited state of the dye to the conduction band of TiO₂ in the picosecond time scale.^{10,11} Efficient electron transfer from the excited dye to the TiO₂ conduction band requires good electronic coupling between the lowest unoccupied orbital (LUMO) of the dye and the Ti 3d orbitals. Effective coupling has typically been accomplished with carboxylate or phosphonate groups, which bind tightly to the TiO₂ surface.

Porphyrins are common photosensitizers because of their very strong absorption in the 400–450 nm region (Soret band) as well as absorptions in the 500–700 nm region (Q-bands). In the present investigation, 5,10,15,20-tetrakis(4-carboxyphenyl)porphyrin (TCPP) is used as the sensitizer (Figure 1). There have been several reports of photosensitizations by ZnTCPP, which is an efficient sensitizer for TiO₂.^{12–15} In this study, we

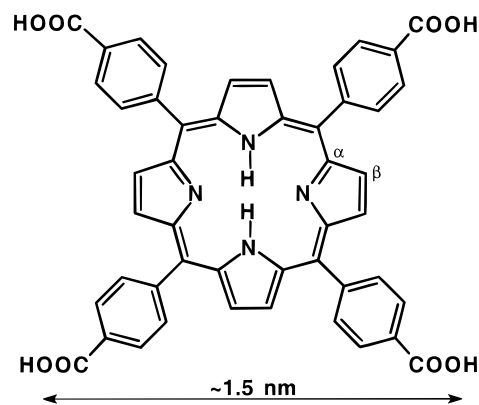


Figure 1. 5,10,15,20-Tetrakis(4-carboxyphenyl)porphyrin (TCPP).

report on the relative effectiveness of TCPP and the nature of its adsorption onto the surface of TiO₂.

Experimental Section

Materials. Nanoparticulate TiO₂ was provided by Degussa.¹⁶ The P25 form is specified to have a nominal particle size of 21 nm, specific surface area of 50 ± 15 m²/g, and a composition of about 70% anatase and 30% rutile. Using the BET method, we measured the surface area of P25 TiO₂ as 55 m²/g. TCPP

and other porphyrins were purchased from Porphyrin Products (Logan, UT) and used without further purification. The ruthenium complex most often used as a dye in Grätzel cells (called N3)² was provided by Mr. Brian O'Regan, University of Washington. Deoxycholic acid (DCA), Triton X-100, acetylacetone, titanium tetrabutoxide, ethylene carbonate, propylene carbonate, 2-propanol, potassium iodide, iodine, and platinum foil (99.99%) were all purchased from Aldrich (Milwaukee, WI) and used as received. The ethanol was absolute grade, from McCormick Distilling Co., Inc. ITO was from Delta Technologies (Stillwater, MN) and was specified to have a conductance of 20 ohms/square and an antireflection coating on the non-conductive side. Scotch tape was standard 3M brand transparent tape with a thickness of 60 μm measured by profilometry.

Electrode Preparation and TCPP Adsorption. Colloidal TiO₂ electrodes were prepared essentially as described by Kay and Grätzel.⁷ The conductive side of a piece of ITO 8 \times 3 cm was treated with a few drops of a 0.01 M solution of Ti(OBu)₄ in *i*-PrOH, allowed to wet completely, and allowed to air-dry. This process is designed to create a compact underlayer of TiO₂ adhering to the ITO electrode. The electrode was then taped down onto a flat surface with standard Scotch tape covering 0.5 cm along each long side. The colloidal paste was prepared by grinding 6 g of TiO₂ in a mortar and pestle with 4 mL of distilled water, 0.2 mL acetylacetone (to minimize reaggregation of the nanoparticles), and 0.1 mL Triton X-100 (to minimize cracking during the sintering process). During grinding, water was occasionally added to maintain the consistency of a thick paste. After at least 30 min of grinding, a few drops of the paste were applied to one end of the taped electrode. A straight, glass rod was used to spread the paste evenly along the electrode, with the Scotch tape determining the thickness and serving as the boundaries. After air-drying, the tape was removed, and the electrode was placed in an oven (Thermolyne 47 900) at 450 °C for 30 min. All of the organic materials were burned off during this treatment and the electrode appeared pure white. After cooling to room temperature, the electrode was cut into 16 pieces of dimension 1.0 \times 1.5 cm. The final electrodes had a 1.0 \times 1.0 cm active (coated) area and a 1.0 \times 0.5 cm uncoated area. These electrodes served as either the photoanode for irradiation studies or the substrate for adsorption or spectroscopic studies. Although the paste was applied at a thickness of about 60 μm (the thickness of the Scotch tape), the sintering process led to substantial densification, and a final thickness of about 14 μm of TiO₂ was measured by profilometry.

To adsorb TCPP onto the TiO₂ electrodes, an electrode was reheated to 450 °C for 30 min to reactivate the surface, then before fully cooling to room temperature (50–80 °C), plunged into 2.5 mL of ethanolic TCPP solution. For the irradiation studies, the concentration was most commonly 0.1 mM TCPP, but a wide range of other concentrations was also used for various studies. The electrode was allowed to sit overnight in the solution, during which the purple color could be seen to have penetrated the electrode uniformly. The TCPP/TiO₂ electrode was withdrawn from solution, allowed to drain onto absorbent paper, and air-dried. Further treatment depended on which types of studies were carried out.

For adsorption studies, initial TCPP solution concentrations ranged from 10⁻⁶ to 10⁻⁴ M. The solution concentrations determined after adsorption was complete (typically overnight) constituted the equilibrium concentration used in the Langmuir adsorption equations. To determine the amount of TiO₂ on a given electrode, the electrode was weighed before and after scraping off the TiO₂. Typically, an electrode contained about

2 mg of TiO₂. Given the 1 cm² area and a measured thickness of 14 μm , the volume of the electrode is 1.4 μL , and its average density is 1.4 g/cm³. Because the density of TiO₂ is about 4 g/cm³ (rutile is 4.2 and anatase 3.9), these values suggest that the electrodes consist of about 65% open space and 35% TiO₂. Electrochemical studies have determined a porosity of about 60%, which is significantly reduced upon dye adsorption.¹⁷

Spectroscopic and Analytical Methods. UV–vis transmission spectra were taken on a Shimadzu model 260 equipped with a GPIB card and a PC for data acquisition and display via Shimadzu UV-265 software. The solution spectra were referenced against the appropriate solvent, and the transmission spectra of the electrodes were referenced against a blank TiO₂ electrode, although such spectra typically gave excessive scattering below about 500 nm.

X-ray photoelectron spectroscopy (XPS) was carried out by Dr. Easo George at Oak Ridge National Laboratories. Deconvolution of the XPS spectral peaks was carried out at Colorado State University by Dr. Rudy Schlaf, using an asymmetrical Gaussian/Lorentzian mixed function.

Resonance Raman Spectroscopy (RRS) was carried out by Dr. Pierre Moenne-Loccoz at the Oregon Graduate Institute using the 457.9 nm line of an Ar-ion laser (Coherent Innova 90-6). The backscattered light was analyzed with a McPherson 2061/207 spectrograph (0.67 m) equipped with a liquid N₂ cooled CCD detector (Princeton Instruments). A Kaiser Optical supernotch filter was used to attenuate Rayleigh scattering. The frequencies were calibrated relative to indene and CCl₄ standards and are accurate to ± 1 cm⁻¹.

Scanning electron microscopy (SEM) was carried out at Portland State University using an ISI SS40 instrument. Atomic Force Microscopy (AFM) was carried out by Dr. David Soltz at Colorado State University using a Digital Instruments Nanoscope III. Profilometry was carried out at the Oregon Graduate Institute using a Sloan Dektak IIA Profilometer. In general, spectral data were imported into Igor Pro (WaveMetrics, Lake Oswego, OR) for data analysis and presentation.

Irradiation Methods. For irradiation studies, the ethanolic 0.1 mM TCPP solution also contained 2 mM deoxycholic acid (DCA) as a coadsorbent, which is considered to help avoid dye aggregation and minimize back-electron transfers by coating otherwise uncovered areas of the TiO₂ surface.⁷ A TCPP/DCA/TiO₂ electrode was mounted against a flat Pt-counter electrode, and the pore spaces were filled by capillary action using a drop of a redox electrolyte consisting of 100 mM KI and 50 mM I₂ in a 80:20 (v/v) solution of ethylene carbonate and propylene carbonate. Irradiation of the cell was provided by the output of a 150 W xenon lamp (PTI) passed through a 20-cm water filter to remove infrared, a monochromator, an optical diffuser, and a short-wave cutoff filter of 400 nm wavelength. The irradiation was always through the transparent working electrode. With the monochromator in zero order, the output approximated the solar spectrum but had an intensity of only about 1.4 mW/cm² (one sun at AM 1.5 is about 100 mW/cm²). Higher intensities were obtained by removing the monochromator. The light intensities were measured with an International Light Instruments ILI 1700 radiometer with a calibrated silicon detector. For white-light irradiation studies, current–voltage curves were obtained by scanning a bias voltage while measuring photocurrents or dark currents with a Keithley 236 source-measure electrometer. Action spectra were obtained by stepping the monochromator through 5 nm increments while measuring short-circuit photocurrents with the electrometer. All of the data

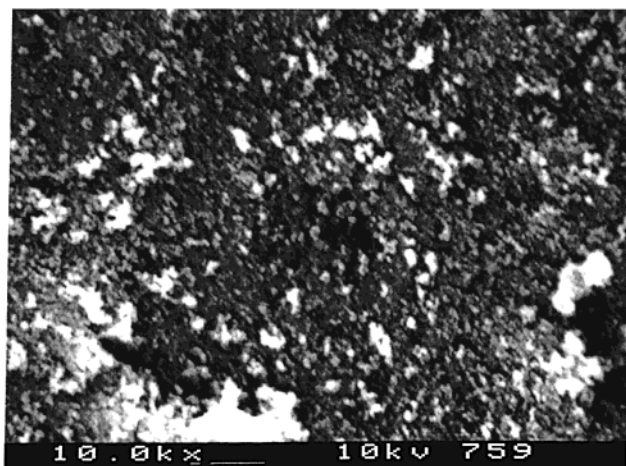


Figure 2. SEM of a typical sintered TiO₂ film (scale bar indicates 1 μm).

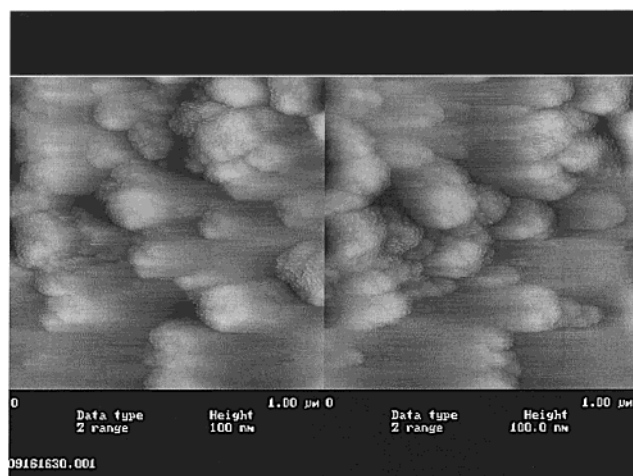


Figure 3. AFM image of a typical sintered TiO₂ film.

acquisition and control were performed by a custom program written in LabVIEW (National Instruments, Austin, Texas).

Results and Discussion

Studies of the TiO₂ Electrodes. The surface morphology of the TiO₂ electrodes was investigated using SEM and AFM. The images shown in Figures 2 and 3 reveal the highly porous nature of the film, consistent with that observed in similar preparations of nanoparticulate TiO₂ electrodes.

Adsorption onto TiO₂ Electrodes. The adsorption of TCP on sintered TiO₂ electrodes and onto freely dispersed TiO₂ particles was studied. The data obtained were plotted (Figure 4) using the equation $C_{eq}/n^s = 1/n_{max}b + C_{eq}/n_{max}$, where C_{eq} is the equilibrium concentration, n^s is the number of moles of solute adsorbed per gram of TiO₂, n_{max} is the total number of moles of adsorption sites available per gram of TiO₂, and b is the adsorption constant.

For the sintered TiO₂ electrodes, this treatment indicates a TCP saturation coverage of 47 μmol/g and an adsorption constant of $b = 9.8 \times 10^4 \text{ M}^{-1}$. For the freely dispersed colloidal TiO₂ particles, a saturation coverage of 77 μmol/g and an adsorption constant of $2.8 \times 10^5 \text{ M}^{-1}$ is calculated.¹⁸ Using an available total surface area of 55 m²/g for TiO₂ in the colloidal suspension (the value specified by the manufacturer and also measured by BET methods for our samples as a dry powder), the average surface area occupied by a TCP molecule at saturation coverage can be calculated to be 1.2 nm²/molecule.

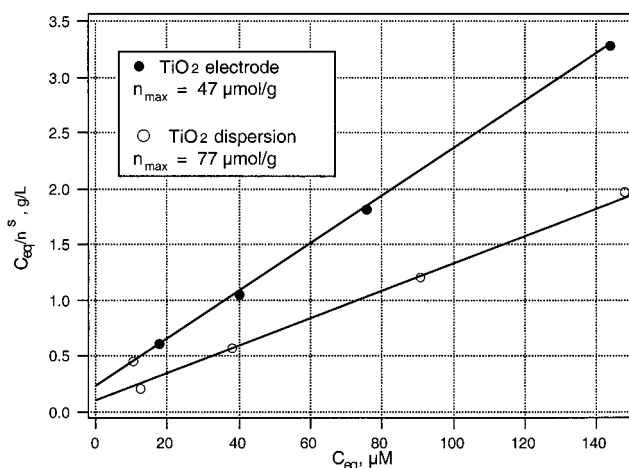


Figure 4. Langmuir adsorption isotherm of TCP in ethanol on sintered TiO₂ electrodes and TiO₂ dispersed colloids.

A TCP molecule lying in a flat geometry would occupy an area of about 2.3 nm², and a well-packed edgewise stacking of TCP would occupy about 0.6 nm² per molecule. We conclude that the observed coverage is due to imperfectly stacked TCP molecules, potentially including a variety of different adsorption modes including multilayers.

The lower saturation coverage for the sintered electrodes, relative to the freely dispersed particles, may be attributed to different adsorption orientations and/or a reduced accessible surface area. We consider the latter most likely, because it has been shown that the sintering process leads to a diminished available surface area. Specifically, anatase TiO₂ particles of surface area 88 m²/g were shown to reduce to 66 m²/g upon heating to 450 °C, presumably due to interconnections made between particles; removing and grinding the sintered material contributed to an increase of 10% in surface area, i.e., from 60 to 66 m²/g.¹⁹ If we consider the 25% decrease in surface area to be caused by the heating to 450 °C, we would predict that the 55 m²/g P25 TiO₂ particles might be reduced to 41 m²/g. Because we did not remove and grind the sintered electrode material, the actual area would be predicted to be about 37 m²/g. The observed value of 47 μmol/g for TCP adsorption on sintered electrodes correlates with a surface area of 34 m²/g, using the same average molecular area of 1.2 nm²/molecule as found for the adsorption on freely dispersed particles. Thus, we believe that TCP adopts the same adsorption orientation(s) onto TiO₂, whether it is as free colloidal particles or as a sintered electrode. This conclusion is based on the calculation, justified above, that Degussa P25, with a nominal surface area of 55 m²/g, actually has only about 34 m²/g of accessible surface area after sintering into a thin-film electrode, as in a Grätzel cell.

Adsorption Irreversibility. The reversibility of the adsorption process was tested by reimmersing TCP/TiO₂ electrodes with various amounts of adsorbed TCP into fresh ethanol solvent. After standing overnight, only a relatively small fraction of TCP was desorbed (10–20%), consistently less than would have been expected based on a true equilibrium. Although consistent values of n_{max} and b were obtained in the adsorption studies, it was not possible to get consistent values from desorption studies. Studies involving insertion of TCP/TiO₂ electrodes into new solutions that contained various TCP concentrations gave either desorption or additional adsorption, depending on the relative solution concentration, but consistent equilibrium data were not obtained with this method either.

TCP can be completely removed from the TiO₂ electrodes by treatment with either aqueous acid or base. In these cases,

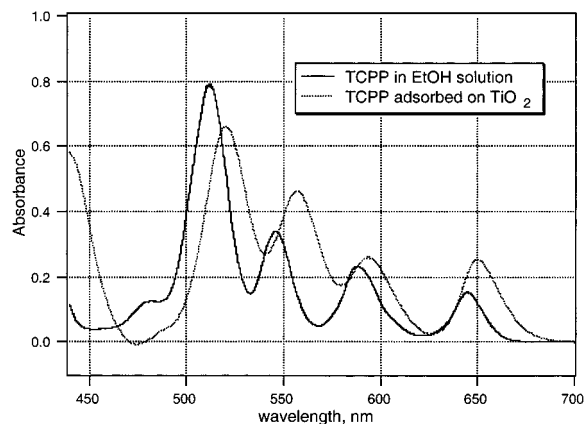


Figure 5. Absorption spectra of TCPP on a TiO₂ electrode and in solution.

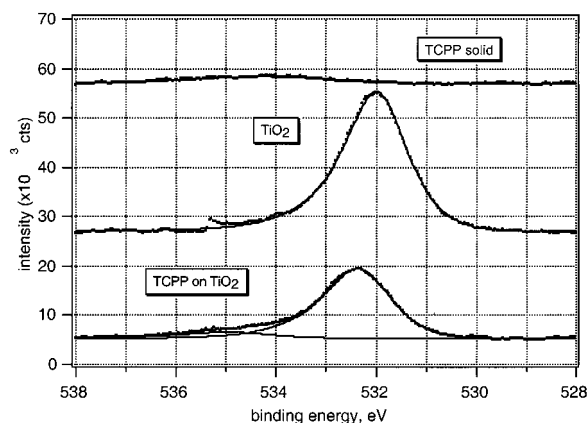


Figure 6. XPS Spectra: O 1s region.

the TCPP and the TiO₂ are charged similarly and electrostatic repulsion leads to complete desorption.

The irreversibility of the adsorption of TCPP suggests that there may be a variety of binding sites, cooperative binding, or other complications that would obviate a classical Langmuir equilibrium approach to the adsorption. Nevertheless, the calculated saturation coverages come from the slopes of the lines in Figure 4, and these are consistent and clearly different. Conclusions about binding constants or multiple binding constants are less clear. Fuller evaluation of the data in Figure 4, combined with more extensive data obtained in our and other laboratories,^{18,20} will be undertaken. Preliminary analysis suggests that cooperative binding may be significant, i.e., interactions with porphyrins already on the surface may contribute to the binding energy. To help elucidate the nature of the binding of TCPP on the surface of TiO₂, we applied a variety of spectroscopic and surface techniques.

UV–Vis Spectroscopy. The electronic absorption spectrum of TCPP in the visible region (the Q-bands) is distinctly red-shifted upon adsorption on TiO₂ (Figure 5). The shift for the two lowest energy bands is about 5 nm (0.5 kcal/mol) and for the two higher-energy bands is about 10 nm (1.0 kcal/mol). The Soret band is difficult to observe because of the extreme light scattering at wavelengths below about 500 nm. In general, tetraphenylporphyrins show a red shift of their Q-bands and a blue shift of their Soret band in more polar solvents.²¹ Apparently, TCPP on TiO₂ (the spectra are taken of dry electrodes) experiences an environment more polar than ethanol.

X-ray Photoelectron Spectroscopy (XPS). XPS was used to distinguish any changes in TCPP or TiO₂ upon adsorption. Because XPS is a highly surface-selective technique, it was

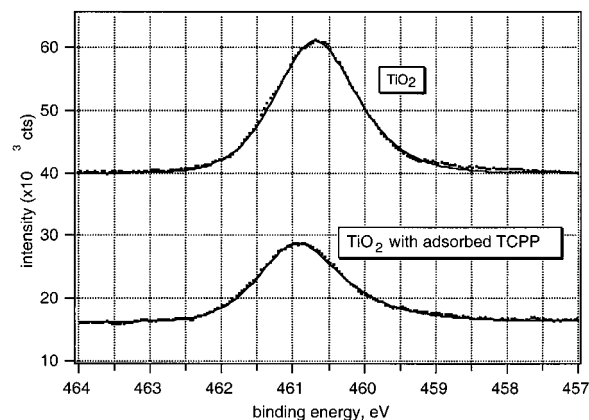


Figure 7. XPS Spectra: Ti 2p_{3/2} region.

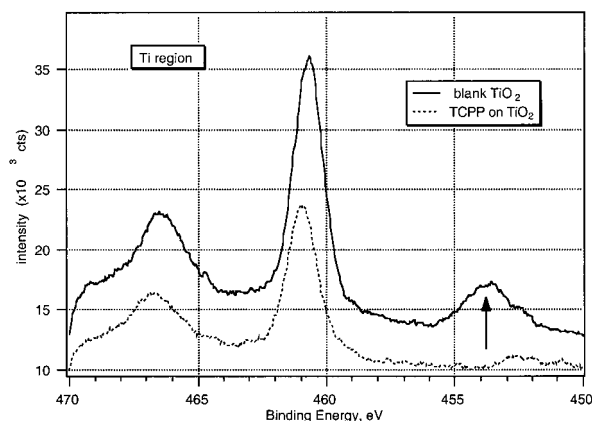


Figure 8. Disappearance of the Ti XPS peak around 454 eV upon adsorption of TCPP.

TABLE 1. Parameters Obtained from Curve Fits of O (1s) and Ti (2p_{3/2}) XPS Peaks

		TiO ₂	TCPP solid	TCPP on TiO ₂
O (1s)	BE (eV)	532.0	534.3	532.4, 535.0
	fwhm	1.54	3.15	1.67, 2.28
Ti (2p _{3/2})	BE (eV)	460.7		460.9
	fwhm	1.40		1.40

expected that different forms of surface or bulk material could be distinguished. The spectra of the Ti (2p) and O (1s) regions are shown in Figures 6 and 7. The samples that were compared included a blank nanocrystalline TiO₂ electrode, pure TCPP, and TCPP adsorbed on TiO₂ (Table 1). The peaks that are attributable to TiO₂ are shifted to higher binding energies by 0.2–0.4 eV upon TCPP adsorption, i.e., both the O (1s) and the Ti (2p_{3/2}) peaks. Similarly, the O (1s) peak, attributable to TCPP, is also shifted to higher binding energy, by about 0.7 eV in this case. Both the N (1s) and the O (1s) peaks of TCPP are shifted; however, there is no indication of a C (1s) shift. These data suggest that there is a substantial interaction between TCPP and TiO₂. Interestingly, one of the Ti peaks that appears clearly in blank TiO₂ at about 454 eV essentially disappears upon adsorption of TCPP (Figure 8). This peak may represent Ti(III) surface states of TiO₂, i.e., sites with ligand vacancies and somewhat higher electron density compared to Ti(IV) in bulk (tetravalent) TiO₂. The location of Ti(III) in the Ti(2p_{3/2}) region has been attributed at approximately this energy.²² Upon adsorption of a new ligand such as TCPP, such states would tend to return to normal valency and any excess electron density would be pushed into the bulk (conduction band). Specific removal of surface states by complexation with adsorbate has been suggested before, based on the observation that the rate

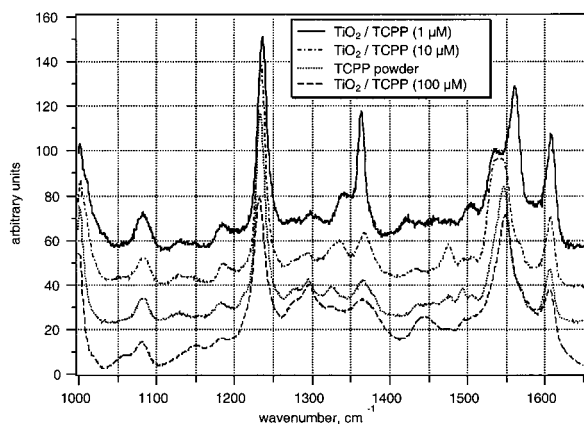


Figure 9. High-frequency region of RRS of TCPD adsorbed from different initial concentrations of TCPD compared to that of solid TCPD.

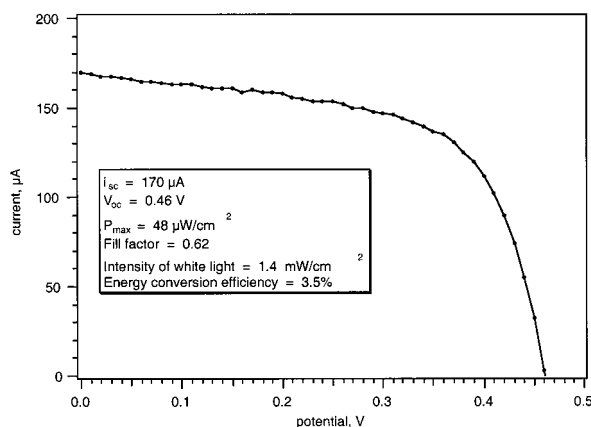


Figure 10. Current–voltage curve of a TCPD-sensitized TiO_2 cell upon irradiation with low-intensity white light simulating the solar spectrum.

of interfacial electron transfer from the conduction band of colloidal TiO_2 to acceptors in solution is greatly enhanced by the adsorption of bidentate benzene derivatives that are adsorbed on the surface of the TiO_2 particles.²³

Resonance Raman Spectroscopy (RRS). RRS was used to identify specific vibrational modes that might indicate the surface interactions between TCPD and TiO_2 . The samples that were studied included pure TiO_2 , pure TCPD, and TCPD/ TiO_2 electrodes prepared by adsorption from ethanol solutions of 1 μM , 10 μM , and 100 μM TCPD. The spectrum of the electrode from 100 μM TCPD was essentially identical to that of pure TCPD, which suggests that TCPD adsorbed from concentrated solutions experiences other TCPD molecules as nearest neighbors, rather than TiO_2 . In contrast, the spectra of electrodes made from dilute solutions of TCPD showed some distinctively different features (Figure 9). In particular, enhanced peaks at 1363 and 1606 cm^{-1} and the splitting of the peak at 1545 cm^{-1} were observed. Assignments based on TSPP and TCPD spectra²⁴ are 1363 ($\text{C}_\alpha\text{--N}$), 1606 (phenyl), 1552 ($\text{C}_\alpha\text{--C}_m$), and 1566 ($\text{C}_\beta\text{--C}_\beta$ and $\text{C}_\beta\text{--H}$).

These data may be compared to the reported spectra of adsorbed tetraphenylporphyrins on an Ag surface, for which TCPD is thought to have a parallel orientation to the silver electrode.²⁴ In another study on the interaction of cobalt phthalocyanine (CoPc) with a silver electrode, the splitting of the 1545 cm^{-1} band was attributed to the interaction of the π orbitals of the phthalocyanine ring with the electrode surface.²⁵ Our study, using RRS, indicates that the adsorption of TCPD onto the TiO_2 film surface shows two effects: at very low coverages, from micromolar solution concentration, TCPD

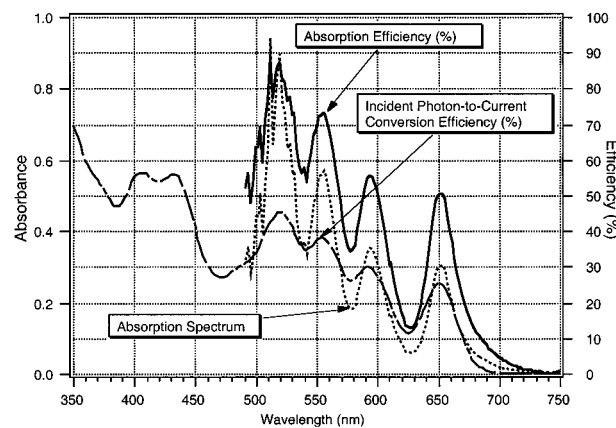


Figure 11. Absorption and action spectra of a TCPD-sensitized cell.

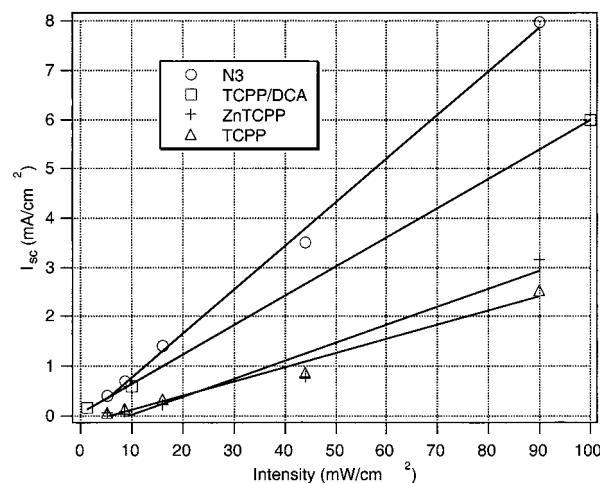


Figure 12. Intensity dependence (white light) of photocurrents from various photosensitizers.

molecules are independent in their interaction with the surface, but as the solution concentration increases, porphyrin–porphyrin interactions are significant. This latter effect occurs well before surface saturation is observed, so the surface orientation of TCPD is likely to be best described as involving significant porphyrin–porphyrin interactions. The Langmuir adsorption studies as a function of concentration also suggest that porphyrin–porphyrin interactions are significant in affecting the binding energy.

Energy Conversion Efficiency. The current–voltage characteristics of an optimized cell, prepared from 0.1 mM TCPD and 2 mM DCA, were determined upon irradiation with white light having an intensity of 1.4 mW/cm^2 ($\sim 1.4\%$ of one sun) (Figure 10). The short circuit current under these conditions (I_{sc}) is 170 μA and the open circuit potential (V_{oc}) is 0.46 V. The maximum power from the cell was found to be 48 $\mu\text{W}/\text{cm}^2$, at 0.36 V and 133 $\mu\text{A}/\text{cm}^2$. The fill factor is 62%, and the overall energy conversion efficiency of the cell is 3.5%.

Action Spectra. Photocurrents generated by the cell were measured as a function of wavelength in the 400–800 nm region. By referencing these to measured incident irradiation intensities at each wavelength, an action spectrum was obtained. Figure 11 plots the incident photon-to-current conversion efficiency, IPCE, versus wavelength as well as the absorption spectrum of an electrode (taken referenced against a blank electrode) in two modes—absorbance and absorption efficiency in percent of incident irradiation intensity. The excessive light scattering below about 500 nm obscures the absorption spectrum. A comparison of the absorption efficiency to IPCE gives an approximate measure of quantum efficiency (i.e., the

photocurrent in electrons per photon absorbed is about 50%), but this does not take into account light losses by reflection or scattering or absorption by the redox electrolyte.

The shape of the action spectrum is slightly broader but clearly follows the shape of the absorption spectrum of TCPP adsorbed on TiO₂. The breadth is due to the wide slits used to maximize the light intensity throughput; mathematically smoothing the absorption spectrum leads to a broadening that more closely approximates the action spectrum.

Light Intensity Dependence. Figure 12 compares the short-circuit photocurrents that are measured upon white-light irradiation of a variety of different dye-sensitized TiO₂ cells. All of the cells were prepared identically, with the exception of the selection of the dye. All of the cells scale linearly with light intensity up to about one sun. The most typical dye used in the Grätzel cell, called N3,² is a superior photosensitizer, but TCPP and ZnTCPP also give excellent results.

Acknowledgment. We thank the U. S. Department of Energy, Basic Energy Sciences, Solar Photochemistry Program, for financial support through Grant No. DE-FG06-90ER-14131. We also thank the Oak Ridge National Laboratory SHARE Program for a travel grant to obtain XPS spectra. We thank Dr. Margie Fyfield (Portland State University) for collaboration on the BET measurements and for the TCPP adsorption measurements in colloidal dispersions. We are grateful to a number of experts who provided assistance with specialized areas: Dr. Pierre Moenne-Loccoz (Oregon Graduate Institute) for Resonance Raman spectra; Dr. Easo George (Oak Ridge National Laboratory) for XPS spectra; Dr. Rudy Schlaf (Colorado State University) for deconvolution of XPS spectra; Professor John Dash (Portland State University) for SEM; and Dr. David Soltz (Colorado State University) for AFM.

References and Notes

- (1) O'Regan, B.; Grätzel, M. *Nature* **1991**, *353*, 737–740.
- (2) Nazeeruddin, M. K.; Kay, A.; Rodicio, I.; Baker, R. H.; Müller, E.; Liska, P.; Vlachopoulos, N.; Grätzel, M. *J. Am. Chem. Soc.* **1993**, *115*, 6382–6390.

- (3) Argazzi, R.; Bignozzi, C. A.; Heimer, T. A.; Castellano, F. N.; Meyer, G. J. *J. Am. Chem. Soc.* **1995**, *117*, 11 815–11 816.
- (4) Kay, A.; Grätzel, M. *Sol. Energy Mat. Sol. Cells* **1996**, *44*, 99–117.
- (5) Hoyle, R.; Sotomayor, J.; Will, G.; Fitzmaurice, D. *J. Phys. Chem. B* **1997**, *101*, 10 791–10 800.
- (6) Bach, U.; Lupo, D.; Comte, P.; Moser, J. E.; Weissortel, F.; Salbeck, J.; Spreitzer, H.; Grätzel, M. *Nature* **1998**, *395*, 583–585.
- (7) Kay, A.; Grätzel, M. *J. Phys. Chem.* **1993**, *97*, 6272–6277.
- (8) Kay, A.; Humphry-Baker, R.; Grätzel, M. *J. Phys. Chem.* **1994**, *98*, 952–59.
- (9) Cherepy, N. J.; Smestad, G. P.; Grätzel, M.; Zhang, J. Z. *J. Phys. Chem. B* **1997**, *101*, 9342–9351.
- (10) Tachibana, Y.; Moser, J. E.; Grätzel, M.; Klug, D. R.; Durrant, J. R. *J. Phys. Chem.* **1996**, *100*, 20 056–20 062.
- (11) Huang, S. Y.; Schlichthörl, G.; Nozik, A. J.; Grätzel, M.; Frank, A. J. *J. Phys. Chem. B* **1997**, *101*, 2576–2582.
- (12) Kalyanasundaram, K.; Vlachopoulos, N.; Krishnan, V.; Monnier, A.; Grätzel, M. *J. Phys. Chem.* **1987**, *91*, 2342–2347.
- (13) Vlachopoulos, N.; Liska, P.; McEvoy, A. J.; Grätzel, M. *Surf. Sci.* **1987**, *189–190*, 823–831.
- (14) Dabestani, R.; Bard, A. J.; Campion, A.; Fox, M. A.; Mallouk, T. E.; Webber, S. E.; White, J. M. *J. Phys. Chem.* **1988**, *92*, 1872–1878.
- (15) Boschloo, G. K.; Goossens, A. *J. Phys. Chem.* **1996**, *100*, 19 489–19 494.
- (16) Degussa Technical Bulletin Pigments No. 56. *Highly Dispersed Metallic Oxides Produced by the AEROSIL Process*; Degussa AG: Frankfurt, Germany, 1990.
- (17) Papageorgiou, N.; Barbe, C.; Grätzel, M. *J. Phys. Chem. B* **1998**, *102*, 4156–4164.
- (18) Fyfield, M. *Electron Microscopy and Adsorption Studies of TiO₂*. Ph.D. Thesis, Portland State University, Portland, OR, 1996.
- (19) Tunesi, S.; Anderson, M. A. *Langmuir* **1992**, *8*, 487–495.
- (20) Cherian, S. *Adsorption and Photosensitization Studies of Porphyrins on Colloidal TiO₂*. Ph.D. Thesis, Portland State University, Portland, OR, 1997.
- (21) Gouterman, M. *Optical Spectra and Electronic Structure of Porphyrins and Related Rings*. In *The Porphyrins*; Dolphin, D., Ed.; Academic Press: New York, 1978; Vol. III; pp 1–165.
- (22) Södergren, S.; Siegbahn, H.; Rensmo, H.; Lindström, H.; Hagfeldt, A.; Lindquist, S.-E. *J. Phys. Chem. B* **1997**, *101*, 3087–3090.
- (23) Moser, J.; Punchedewa, S.; Infelta, P. P.; Grätzel, M. *Langmuir* **1991**, *7*, 3012–3018.
- (24) Cotton, T. M.; Schultz, S. G.; Duynes, R. P. V. *J. Am. Chem. Soc.* **1982**, *104*, 6528.
- (25) Kötz, R.; Yeager, E. *J. Electroanal. Chem.* **1980**, *113*, 113.